

# Influences of Molecular Weight and Particle Morphology on Film Processing Properties of Polyvinyl Fluoride

Jing Wang, Yafei Lu, Hongfei Li, Huilin Yuan

*The Key Laboratory of Beijing City for Preparation and Processing of Novel Polymer Materials, Beijing University of Chemical Technology, Beijing 100029, China*

Received 9 September 2005; accepted 18 March 2006

DOI 10.1002/app.24451

Published online in Wiley InterScience (www.interscience.wiley.com).

**ABSTRACT:** To select a suitable kind of resin for preparing films, the melting point ( $T_m$ ), thermal decomposition temperature ( $T_d$ ), and stretch property of polyvinyl fluoride (PVF) as a function of the viscosity-average molecular weight ( $M_\eta$ ) were investigated. The results showed that  $T_d$  and maximal stretch ratio of extrusion-cast PVF films gradually increase with the increase of  $M_\eta$ .  $T_m$  also increases when  $M_\eta$  is below 400,000, but keeps invariable when  $M_\eta$  is beyond 400,000. Six different kinds of PVF resin samples in this article were classified into three types, according to their particle morphologies: (1) loose-structured PVF (PVF-A and G); (2) tight-structured PVF (PVF-F); and (3) intermediate-structured PVF (PVF-B, E, and H). The effects of the morphology on the solvent absorbability of PVF were

studied. The results indicated that the loose-structured PVF has better absorption capacity to solvent than does tight-structured PVF. The processing temperature can be considerably reduced when *N,N*-dimethylformamide (DMF) as a plasticizer was mixed with PVF, and the diminished magnitude depends on the absorption capacity of PVF to DMF. The evaporation of DMF is influenced by both molecular weight and particle morphology of PVF, and the final residue of DMF in the PVF/DMF mixture is dependent on the molecular weight of PVF. © 2006 Wiley Periodicals, Inc. *J Appl Polym Sci* 102: 1780–1786, 2006

**Key words:** polyvinyl fluoride; film; molecular weight; particle morphology; processing property

## INTRODUCTION

It is well known that polyvinyl fluoride (PVF) has good properties, such as excellent resistance to outdoor weathering exposures, a high degree of physical toughness, chemical inertness, transparency, and retention of properties at both low and elevated temperatures in the film form.<sup>1</sup> PVF has wide applications in aviation, architectural decoration, anticorrosion, agriculture, and food packing, and is a kind of excellent engineering plastic that is indispensable in industry.<sup>2</sup>

Although PVF is one of the thermoplastic polymers, it has high melting point and viscosity. The melting behavior of PVF is always accompanied by the partial decomposition of PVF in air. As a result, the melt processing of PVF becomes quite difficult, and the PVF film manufacture has been limited to solvent-extruded method, which requires high boiling point solvents as processing aids.<sup>3</sup> By far, a great deal of researches on the production and properties of PVF films have been carried out, but only Du Pont Co. has PVF film products with the brand of TEDLAR.<sup>4</sup>

The difficulties in the film process lead to a limitation in the production and applications of PVF films. Therefore, it is very significant and meaningful on how to improve the PVF process technology. The advanced preparing methods of PVF films were described in a few of the patents.<sup>1,5,6</sup> However, it is a notable fact that the differences of the molecular weight, particle morphology, and microstructure of PVF resins, which is due to the diversity of synthetic conditions,<sup>7</sup> have the potential influence on the processing properties of PVF films. Therefore, the investigation on the correlation between the characteristics of PVF resins and film processing properties is not only theoretically significant, but also beneficial to optimize the performance of PVF films. Simril and Curry<sup>8</sup> have proved that the film prepared by using high-molecular-weight PVF has provided with more excellent toughness, higher tensile strength and flexibility, and better resistance to outdoor weathering. Lu<sup>9</sup> studied the particle morphology and microstructure of PVF resin by SEM. But, there has been little work toward establishing the relationship between the molecular weight and morphology of PVF and the film processing properties.

The present work is aimed at understanding the effects of the different characteristics of PVF resins on the film processing properties and finding out the optimal resin to fit for the film production.

Correspondence to: H. Yuan (2004080072@grad.buct.edu.cn).

## EXPERIMENTAL

### Materials and chemical agents

Six PVF resin samples used in this study were obtained from Zhejiang Lantian Environmental Protection Material Co. (Hangzhou). PVF resin was synthesized by the suspension polymerization of the fluoroethylene (VF) monomer in a deionized water medium, with 2-methylpropionamide dihydrochloride as the initiator, at the temperature range from 60 to 70°C. The different characteristics of PVF resins result from the simultaneous varieties of several technological parameters. According to different polymerization conditions, these six different samples were named as PVF-A, PVF-B, PVF-E, PVF-F, PVF-G, and PVF-H (white powder), respectively. *N,N*-dimethylformamide (DMF, the boiling point of 153°C at 101.3 kPa), with the purity of 99.5%, was used as the solvent in this study.

### PVF films' formation

PVF resins were dried at 85°C for 4 h in a vacuum oven (DL102, Tianjin) prior to mixing. The compounds of resins and solvents, with the different mass ratio of resin/solvent, which depended on the solvent absorbability of PVF, were prepared in a high-speed mixer (GH10, Beijing). The mixing conditions were the same for all samples, with the temperature of 60°C, rotational speed of the stirring paddles of 1500 rpm, and mixing time of 10 min. After mixing, the compounds were immediately sealed in glass containers. Three days were needed to ensure that the solvents would completely penetrate into PVF resins. Then the compounds were extruded via a 30-mm Brabender single-screw extruder (PLD651, Germany) equipped with a 160-mm wide sheet casting T-die head. The extruding speed was 30 rpm, and the set temperatures of the head section varied from 130 to 170°C corresponding to the different kinds of PVF resins. The melt extrudates were quenched into a water bath at 23°C to form solvent-containing PVF films. Then the films were passed from the water bath into a stretching apparatus, and the tensile force applied on the films was provided by the clamp force between the first and second roll of the stretching apparatus. The tensile direction was parallel to the extrusion direction of extrudate. Longitudinal stretch ratio can be controlled by varying the rotational speed of the stretcher. Thereafter, the stretched films were dried by subjecting the films under tension, to restrict any dimensional change to a stream of air at a temperature of about 160°C for about 20 min.

### Viscosity average molecular weight

The intrinsic viscosities ( $[\eta]$ ) of the different PVF resins were determined in an Ostwald viscosimeter

(model 1840 with a capillary of 0.6-mm inner diameter) at 90°C in DMF solution. The viscosity average molecular weight ( $M_{\eta}$ ) was calculated according to the following relationship<sup>10</sup>:  $[\eta] = 6.52 \times 10^{-5} M_{\eta}^{0.80}$ .

### Thermal measurements

Differential scanning calorimetry (DSC, from 30 to 250°C) and thermogravimetric (TG, from 40 to 600°C) measurements were performed at a heating rate of 10°C/min under nitrogen atmosphere, by using the model STA-449C thermal analyser (NETZSCH Company).

### X-ray diffraction analysis

X-ray diffraction (XRD) analysis was used to determine the degree of crystallization of PVF. XRD patterns of PVF were recorded on a Rigaku D/max-2500B2+/PCX system, using Cu-K $\alpha$  radiation ( $\lambda = 1.5406$ ) over the range of 5–50 degrees (2 $\theta$ ) at room temperature. The generator was operated at 40 kV and 200 mA.

### Morphology observations

For the morphology characterization, the preparation of the samples included the following steps: (1) put 10 mL of 99.5% ethyl alcohol into a glass beaker with 1 g of PVF resin and stir via an ultrasonic wave, until it disperses uniformly; (2) take a few drops of suspending liquid on the specimen platform with pipette; (3) after the solvent is completely volatilized, the morphology of PVF samples was observed by using a scanning electron microscope (SEM, JSM-6360LV, Japan). During the observation, at least 10 particles of each kind of resin were chosen at random from the specimen platform. The magnifications were listed in the respective photomicrographs, and those magnification factors were calibrated using a grid-spacing standard.

### BET surface area measurements

BET surface areas of PVF-A, B, and F particles were analyzed by a Micromeritics ASAP2020 surface area and porosity analyzer. The samples were outgassed at 150°C for 10 h. Nitrogen (99.99%) was used as an adsorptive. Pore volumes of different samples can be obtained when  $P/P_0$  equals to 0.99, from which the porosity (ratio of the volume of open pores to the total volume of the solid) can be calculated.

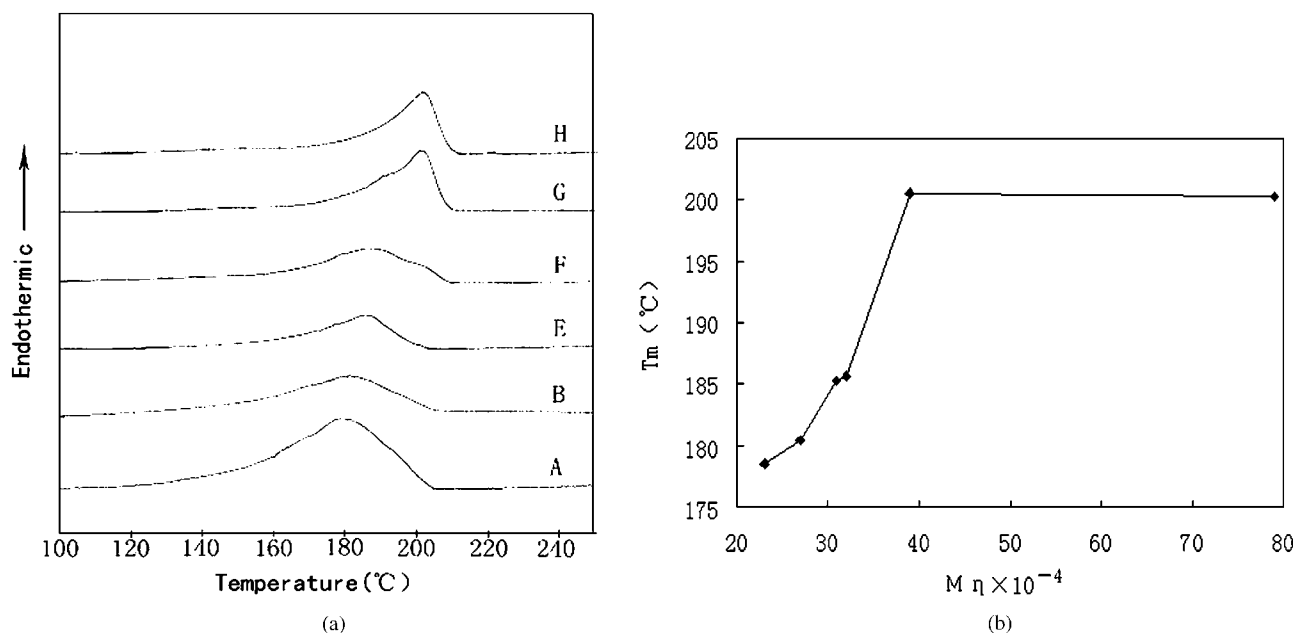


Figure 1 (a) DSC heating thermograms and (b) melting peak temperatures versus molecular weight of PVF resins.

### Solvent absorbability

Referring to the Standard of ISO 4608-1984, the solvent absorbabilities of the different PVF resins were determined in a centrifuger (TGL - 16G) at room temperature. Some of the operation steps in the original standard had been modified considering the characteristics of the PVF resins. First, 0.5 g samples of different PVF resins were put into different centrifugal tubes, followed by dropping excessive DMF solution into each tube. Twenty minutes later, the quantity of solvent was adjusted, and the liquid level was kept at 4 mm higher than the solid level. After the mixtures were treated in the centrifuger at a speed of 10,000 rpm for 30 min, the residual solvent was removed carefully, and then the wall of the tubes was cleaned. The solvent absorbability could be calculated from the following relationship:

$$\text{Solvent absorbability (\%)} = [(m_2 - m_1)/m] \times 100$$

where  $m$ ,  $m_1$ , and  $m_2$  represent the weight of original PVF, PVF plus centrifugal tube, and solvent-absorbed PVF plus centrifugal tube, respectively. The final data were obtained from the averages of three test results.

### Solvent evaporation

Ten gram of PVF resin and DMF were mixed with the mass ratio of resin/solvent = 100/120 in the high-speed mixer. The mixing conditions were the same as described in the previous films' formation part. Place the compounds on the watch glasses uniformly and obtain their total weight, then put them

into an air-blast oven at 153°C (boiling point of DMF). The samples were weighted, until the weight did not change anymore.

## RESULTS AND DISCUSSION

### The influence of molecular weight on the film processing properties

#### Melting temperatures

The DSC heating thermograms of PVF and the variation of melting peak temperatures as a function of  $M_n$  were shown in Figure 1. The values of  $M_n$  and  $T_m$  were listed in Table I. As can be seen from the DSC curves in Figure 1(a), the melting peak of PVF resins became sharper and sharper with the increase of  $M_n$ . That is to say, the fusion temperature range of higher-molecular-weight PVF is narrower than that of lower-molecular-weight PVF.

It can be found in Figure 1(b) that the  $T_m$  of PVF remarkably increased with the increase of  $M_n$  when the  $M_n$  was below 400,000, but they were almost

TABLE I  
Effects of Molecular Weight on the Various Properties of PVF Resins

	Samples of PVF					
	A	B	E	F	G	H
$M_n$ ( $10^{-4}$ )	22.8	26.6	31.3	32.0	38.7	79.0
$T_m$ (°C)	178.5	180.5	185.3	185.7	200.6	200.3
$T_d$ (°C)	379.0	404.5	413.1	414.2	418.9	421.6
Crystallinity $\pm 2$ (%)	54	56	60	60	67	68
Maximal stretch ratio	1.5	2.0	2.7	3.0	4.0	6.0

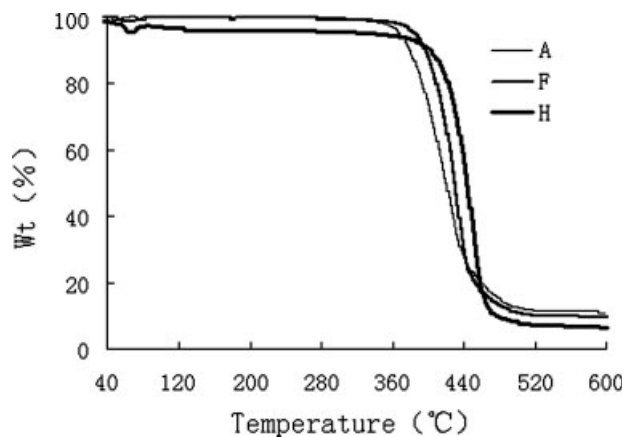


Figure 2 TG curves of three kinds of PVF resins with different molecular weights.

kept invariable when  $M_n$  was beyond 400,000. This phenomenon should be in connection with the crystallinity of PVF listed in Table I. It can be found that the higher the degree of crystallization the higher was the  $T_m$  value. This indicates that the higher-molecular-weight PVF may form more relative perfect crystals, which led to a narrower melting peak and a higher melting point. Besides, the broadening of the melting peaks may also result from a low polydispersity index in PVF, and this topic will be discussed further in our forthcoming study.

Thermal stability

Figure 2 showed the TG curves of three kinds of PVF resins whose molecular weights were very different. It can be found that the PVF samples heated in nitrogen showed one-step decomposition thermo-

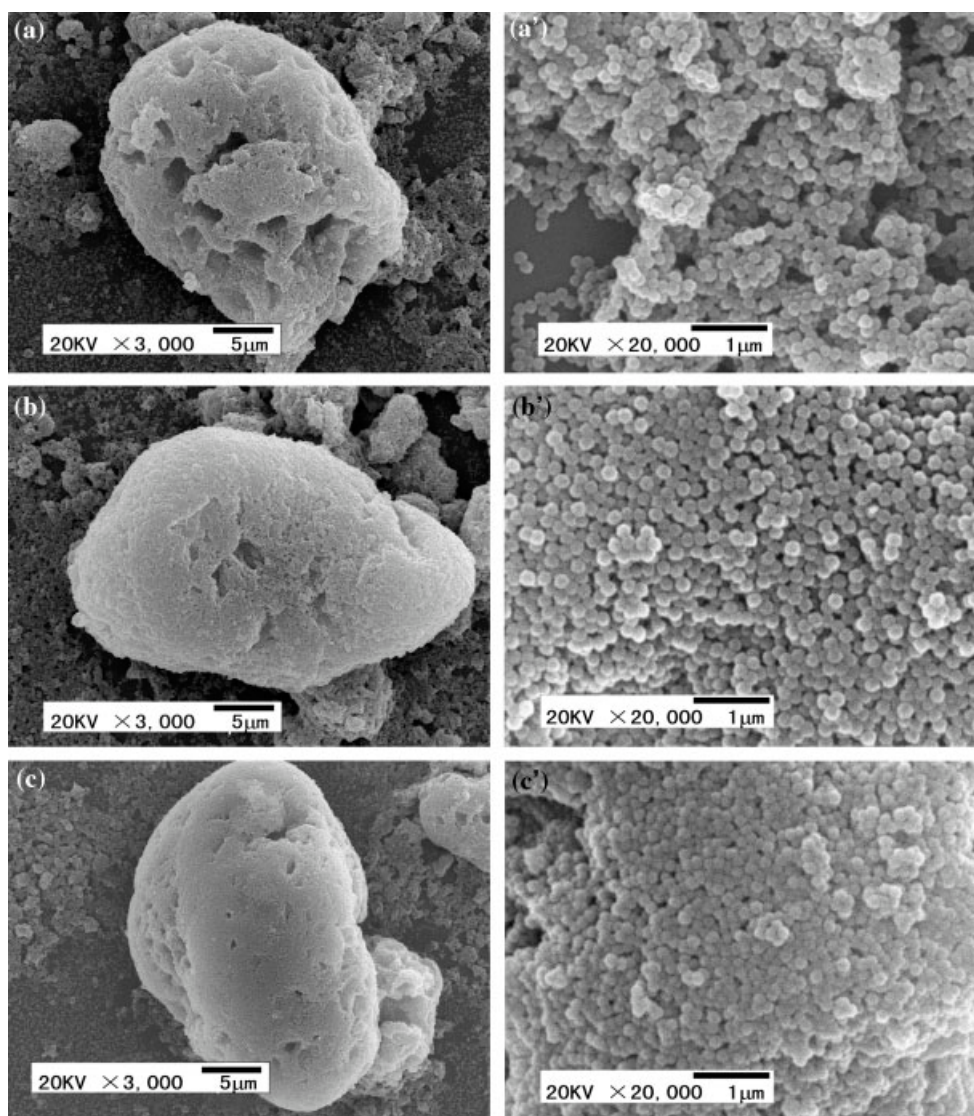


Figure 3 Three types of particle morphology of PVF resins: a,a'-PVF-A, b,b'-PVF-B, c,c'-PVF-F.

**TABLE II**  
Analytical Data of Six Kinds of PVF Resins

	Samples of PVF					
	A	B	E	F	G	H
$M_n (10^{-4})$	22.8	26.6	31.3	32.0	38.7	79.0
BET surface area ( $m^2/g$ )	21.18	12.91	—	7.05	—	—
Porosity (%)	20.8	9.5	—	6.0	—	—
Solvent absorbability $\pm 5$ (%)	232	190	196	178	222	192
Processing temperature ( $^{\circ}C$ )	130	150	155	165	165	170
Final solvent residue <sup>a</sup> (g)	1.6	2.0	2.7	3.0	3.9	4.2

<sup>a</sup> The final solvent residue equals the residual weight of PVF/DMF mixture minus the weight (10 g) of PVF in the mixture.

gram. This result was similar to the experimental conclusions described by Rosenberg et al.<sup>11</sup> They reported that PVF degraded with concurrent hydrogen fluoride loss and backbone cleavage at a certain temperature. In addition, the thermal decomposition temperature ( $T_d$ ) of PVF rose obviously according to the increment of molecular weight. As can be seen from Table I, the  $T_d$  value of PVF-H was  $42^{\circ}C$  higher than that of PVF-A. This result indicates that the thermal stability of the high-molecular-weight PVF is better than that of the low-molecular-weight PVF.

#### Stretch ratio

The highly oriented PVF films are better with respect to the tensile, impact, and burst strengths. The less-oriented PVF films are better with respect to the tear strength and lack of shrinkage at high temperatures.<sup>12</sup> Therefore, the stretch ratio is one of the most important factors influencing the properties of PVF films.

Besides external temperature, molecular weight of PVF is also a critical factor that greatly affects the stretch ratio of extrusion-cast films. Table I showed the maximal stretch ratio (the stretch ratio of the film at the breaking point in longitudinal direction) of extrusion-cast PVF films. It can be found that the maximal stretch ratio of PVF films significantly increased with increasing molecular weight. This phenomenon mainly arises from the characteristic of PVF. Unlike many other normally crystalline thermoplastic polymers, PVF apparently cannot be obtained from the amorphous state by rapidly quenching at the temperature above its crystalline melting point.<sup>1</sup> Instead, PVF with a certain degree of crystallization can be obtained. Usually, with the increment of molecular weight of a crystalline polymer, the amount of engagement chains between crystallites increases,<sup>13</sup> which would retard the break of films at the same stretching force. Therefore, the high-molecular-weight PVF had higher maximal stretch ratio.

#### The influence of particle morphology on the film processing properties

##### Solvent absorbability

According to the accumulated density and form of primary particles with the size range from 0.15 to 0.25  $\mu m$ , PVF can be roughly classified into three types: (1) loose-structure characterized with irregular and coarse surface of accumulated particles, like PVF-A and G; (2) tight-structured characterized with sound and smooth surface of accumulated particles, like PVF-F; and (3) intermediate-structure, like PVF-B, E, and H. So PVF-A, B, and F were taken as three different examples of morphology, and their typical SEM micrographs were shown in Figure 3.

The surface area and porosity are important parameters used to characterize the porous structure of particles. To further verify the differences in the interior structure and morphology of particles, the BET surface area and porosity of PVF-A, B and F measured were given in Table II. As can be seen, the surface area of loose-structured PVF-A was three times more than that of tight-structured PVF-F, and that of intermediate-structured PVF-B was intermediate. The porosity showed the same variation tendency as the surface area. It is understandable that surface area and porosity are comparatively higher in loose accumulated particles because of more and bigger pores in both outside and inside of those particles. The results were consistent with particle morphology, as shown in the SEM micrographs (Fig. 3).

As shown in Table II, the solvent absorbability of different PVF resins did not connect with their molecular weight, but connect with their particle morphologies. The solvent absorbability of sample PVF-A, B, and F, during the same time, was sequentially reduced. Combined with the SEM micrographs, surface area, and porosity data, it can be found that the loose-structured PVF is adaptive to absorb more solvent, and the rate of absorption is higher than the tight-structured PVF.

Different states of PVF resins with different solvent absorbability after mixing with DMF were observed. In case of sample A and F, as shown in Figure 4, the

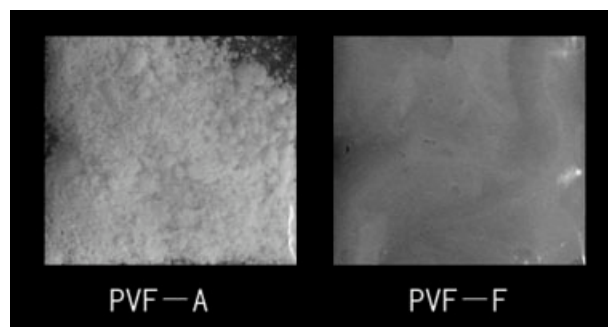


**Figure 4** Photos of the compounds of PVF-A and PVF-F with 120 phr of DMF.

compound of PVF-A and 120 phr of DMF looked like moist sands and felt a little greasy, but the compound of PVF-F and 120 phr of DMF was like a kind of dilute paste. This is another evidence for the excellent solvent absorbability of loose-structured PVF.

Processing temperatures

From Table II, though processing temperatures of PVF resins were still incremental with the increasing molecular weight, the comparison between the melting temperatures of PVF and the processing temperatures (the set temperatures of head section of extruder) of PVF plasticized with DMF, as shown in Figure 5, showed that DMF used as the plasticizer can effectively decrease the processing temperature of PVF. In case of sample PVF-A and PVF-F, it can be found in Table II that the processing temperature of loose-structure PVF-A was 35°C lower than that of the tight-structured PVF-F. The results indicated that the loose-structured PVF particles are more prone to break up and melt than tight-structured PVF particles, after absorbing a great deal of solvent. Meanwhile, in the course of processing, PVF-A exhibited better plasticity and pliability, while the melt viscosity was obviously reduced. However, for the tight-structured PVF-F, the solvent could not completely permeate between the PVF molecules, and most of the solvent was attached to the exterior of the PVF particles, which led to a decrease in the friction and shear heat among particles and the increase of processing temperature.

Solvent evaporation

The swelling behavior of PVF in various solvents has been investigated by Chapiro et al.<sup>14</sup> It was found that solvents can diffuse and insert between PVF molecules by virtue of the osmotic pressure,

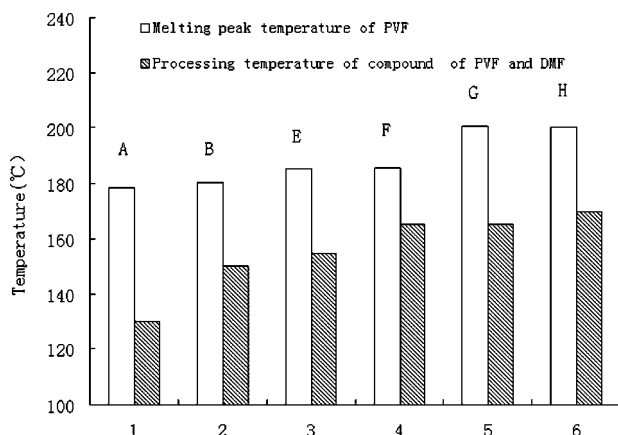


Figure 5 Comparison between melting and processing temperatures of six kinds of PVF resins.

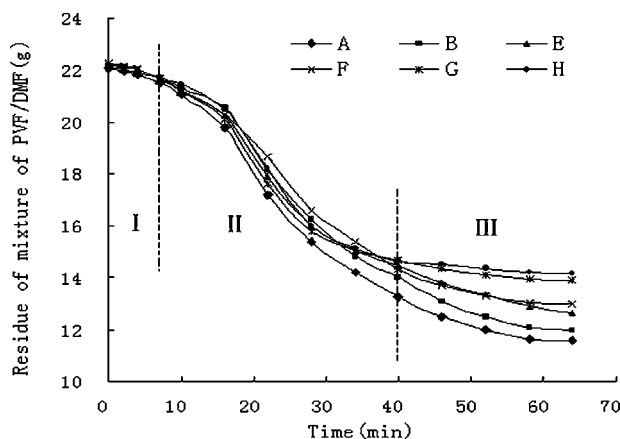


Figure 6 Residue of PVF/DMF compounds as a function of time at 153°C.

meanwhile C—F...F—C dipoles are separated and the “free” C—F dipoles couple with the dipoles of the solvent. Equilibrium swelling is reached when the osmotic pressure equals to the sum of all binding forces between macromolecules. Once the osmotic pressure disappears, the solvent evaporates rapidly from the swollen polymer.

As shown in Figure 6, the evaporation curves of DMF in the mixture of PVF/DMF were separated into three parts. The first part of the curves (up to about 8 min), which were almost superimposed, represented the evaporation of the particle-exterior solvent. Growing solvent loss from ~ 8 to 40 min was related to the evaporation of the particle-interior solvent. It can be seen that the elimination of solvent in PVF/DMF samples was dependent of the particle morphology of PVF resins. The solvent loss was faster in the loose-structured PVF-A than in the tight-structured PVF-F. The reason is that the volatilization resistance in high-porosity particles is least, and there is more free solvent inside the loose accumulated PVF-A particles. In the third part of the curves, which involved the evaporation of intermolecular solvent, the weights of PVF/DMF samples gradually tended to be invariable, but the final solvent residues were pretty different and in direct proportion relations with the molecular weight of polymers. As can be seen from Table II, the higher the molecular weight the higher was the final solvent residue. The phenomenon may result from stronger intermolecular force and exceeding entanglement between the molecular chains of high-molecular-weight PVF, which inhibit the evaporation of intermolecular solvent.

CONCLUSIONS

From the experimental results, the following results can be concluded: (1) the DSC and TG results confirm that the melting temperature and thermal stabil-



ity of PVF really depend on the molecular weight, but the effect of the molecular weight on melting temperature is obvious only when the molecular weight is below 400,000; (2) the maximal stretch ratio of extrusion-cast PVF films, at the same temperature, is significantly increased with the increment of molecular weight; (3) SEM and BET results demonstrate that there is a close correlation between the particle morphology and the solvent absorbability of PVF. Furthermore, the particle morphology and the solvent absorbability of PVF highly affect the processing temperature of PVF films; and (4) the evaporation of DMF mixed into PVF is correlated with both the particle morphology and molecular weight of PVF.

The authors thank Zhejiang Lantian Environmental Protection Material Co. for supplying with PVF resins through project.

## References

1. Prengle, R. S.; Richards, R. L. U.S. Pat. 3,139,470 (1964).
2. Liang, B. *J Mater Eng* 1994, 11, 13 [in Chinese].
3. Stallings, J. P.; Paradis, R. A. *J Appl Polym Sci* 1970, 14, 461.
4. Chen, X. J.; Li, M. W.; Lou, C. Q.; Ni, J. S.; Zhang, Y. X. In *Encyclopedia of Chemical Industry*, Vol. 1: Resins and Plastics; Editorial Committee, Chem Ind Press: Beijing, 2003; Chapter 9 [in Chinese].
5. Bottorf, D. T.; Hecht, J. L.; James, V. E. U.S. Pat. 3,081,208 (1963).
6. Bartron, L. R. U.S. Pat. 2,953,818 (1960).
7. Kalb, G. H.; Coffman, D. D.; Ford, T. A.; Johnston, F. L. *J Appl Polym Sci* 1960, 4, 55.
8. Simril, V. L.; Curry, B. A. *Mod Plast* 1959, 36, 121.
9. Lu, X. M. *Zhejiang Ind* 1984, 15, 55 [in Chinese].
10. Wallach, M. L.; Kabayama, M. A. *J Polym Sci* 1966, 4, 2667.
11. Rosenberg, Y.; Siegmann, A.; Narkis, M.; Shkolnik, S. *J Appl Polym Sci* 1992, 45, 783.
12. Simril, V. L.; Curry, B. A. *J Appl Polym Sci* 1960, 4, 62.
13. Ruan, Y. P.; Cha, L. L. *Guangdong Plast* 2004, 8, 34.
14. Chapiro, A.; Mankowski, Z.; Schmitt, N. *J Polym Sci* 1982, 20, 1791.